A Novel WCS-SFDTD Method for Solving Oblique Incident Wave on Periodic Structures

Y.-F. Mao [1], B. Chen [2], X.-X. Yin [1], and J. Chen [1]

[1] China Satellite Maritime Tracking and Control Department, Jiangyin, 2144000, China
myf4494@163.com, yinxiaoxu@163.com, jianchen73@163.com

[2] National Key Laboratory on Electromagnetic Environment and Electro-optical Engineering
PLA University of Science and Technology, Nanjing, 210007, China
emcchen@163.com

Abstract ─ In this paper, a novel weakly conditionally stable spectral finite-difference time-domain method is proposed to solve oblique incident wave on periodic structures, namely NWCS-SFDTD. Because the stability condition is determined only by one space discretization, this new method is extremely useful for periodic problems with very fine structures in one or two directions. By using the constant transverse wave-number (CTW) wave, the fields have no delay in the transverse plane, as a result, the periodic boundary condition (PBC) can be implemented easily for oblique incident wave. Compared with the alternating-direction-implicit SFDTD (ADI-SFDTD) method this NWCS-SFDTD method has higher computational efficiency and better accuracy, especially for larger time-step size case. At each time step, it only needs to solve four implicit equations and four explicit equations, which is six implicit equations and six explicit equations in the ADI-SFDTD method. So while maintaining the same size of the time-step, the CPU time for this method can be reduced to about two-thirds of that for the ADI-SFDTD method. Numerical examples are presented to demonstrate the efficiency and accuracy of the proposed algorithm. To reduce the numerical dispersion error, the optimized procedure is applied.

Index Terms─ Finite-difference time-domain (FDTD), oblique incident, periodic structure, and weakly conditionally stable.

I. INTRODUCTION

The finite-difference time-domain (FDTD) technique is a robust analysis tool applicable to a wide variety of complex problems [1, 2]. Frequently, problems are encountered in which periodicity exists in one or more dimensions of the problem geometry, taking advantage of this periodicity can lead to greater efficiency and accuracy when solving the problem numerically. Instead of analyzing the entire structure, only a single unit cell needs to be analyzed by incorporating the periodic boundary condition (PBC) [3-5]. For a normally incident wave, the PBC is quite straightforward as there is no phase shift between each periodic cell [1]. However, when a plane-wave source is obliquely incident, there is a cell-to-cell phase variation between corresponding points in different unit cells which causes the time-domain implementation to become more difficult. To deal with this problem, several methods have been introduced, such as the Sine-Cosine method [6] and the split-field method [7]. Recently, another new formulation, named spectral FDTD (SFDTD) was proposed [8], because the constant wave-number (CTW) wave is used, there is no delay in the transverse plane and the PBC can be implemented directly in the time domain.

Aforementioned FDTD methods for periodic structures are explicit time-marching techniques that are subject to the Courant-Friedrich-Levy (CFL) stability condition [1]. As a result, a maximum time-step size is limited by the minimum cell size in a computational domain,

Submitted On: Dec. 11, 2012
Accepted On: Jan. 27, 2014

which makes this method inefficient for the problems where fine-scale structures are involved. To overcome the restriction of the CFL stability condition, an alternating-direction-implicit (ADI) FDTD solution for periodic structures is proposed [9], as well as locally-one-dimensional (LOD) FDTD [10]. Although the time-step size in the ADI-FDTD simulations is no longer bounded by the CFL criterion, the method exhibits a splitting error associated with the square of the time-step size [11], which limits the accuracy of the ADI-FDTD method. Meanwhile, in the ADI-FDTD scheme, it must solve six implicit updates and six explicit updates for one full-update cycle, which makes it computationally inefficient.

To overcome the drawbacks of the ADI-FDTD method, a hybrid implicit-explicit (HIE) FDTD method was submitted [12], and it has been introduced to solve periodic problems [13]. This method has higher accuracy and efficiency than the ADI-SFDTD method, but with confined usage, because the time-step size in this method is limited by two space discretizations, namely, $\Delta t \le 1/\left(c\sqrt{1/\Delta y^2 + 1/\Delta z^2}\right)$, which is independent of Δx. So if there are fine structures in the x-direction, the advantage of the method is obvious. However, for certain problems, if there are fine structures in two directions its efficiency is reduced. Recently, a novel weakly conditionally stable (NWCS) FDTD method, which is extremely useful for problems with very fine structures in two directions was discussed [14], namely, NWCS-FDTD. It has been introduced to the body-of-revolution FDTD [15].

In this paper, the novel weakly conditionally stable technique is applied to the SFDTD method, resulting in a NWCS-SFDTD method, which can solve periodic structures with oblique incident wave efficiently. The time-step size in this method is only determined by one spatial increment, the weakly conditional stability is presented analytically. To eliminate the time delay in transverse plane, the CTW wave [8] is applied. As a result, the FDTD code needs to be changed from real variables to complex variables, which is different from the conventional NWCS-FDTD method. Compared with the ADI-SFDTD method it only needs to solve four implicit updates, other four equations can be updated directly, which are six implicit updates and six explicit updates in the ADI-SFDTD method. The proposed method has higher computational efficiency and better accuracy than the ADI-SFDTD method. The running time can be reduced to about two-thirds of the ADI-SFDTD method. Numerical examples are conducted to verify the accuracy and the efficiency of this implementation. In order to reduce the numerical dispersion error, the optimized procedure is applied.

II. THEORY

A. Spectral FDTD implementation

In the SFDTD method, the incident wave is represented in the frequency domain. By applying an inverse Fourier transform on it, we can obtain the CTW wave in the time domain, which can be represented as [8],

$$\begin{aligned} E_t^{CTW} &= \exp\left(\tilde{j}k_x x\right)\exp\left(\tilde{j}k_y y\right)\xi^{-1}\left[\exp\left(\tilde{j}k_z\left(z-z_0\right)\right)\exp\left(-k_0^2/\sigma^2\right)\right] \\ H_l^{CTW} &= \exp\left(\tilde{j}k_x x\right)\exp\left(\tilde{j}k_y y\right)\xi^{-1}\left[\exp\left(\tilde{j}k_z\left(z-z_0\right)\right)Y_{TE}\exp\left(-k_0^2/\sigma^2\right)\right] \\ Y_{TE} &= k_z/\eta_0 k_0 \end{aligned} \tag{1}$$

where k_x, k_y represent transverse wave-numbers, which are assumed to be constant numbers (independent of frequency). k_z is normal wave-number, $k_0 = 2\pi f/c$, and $\tilde{j} = \sqrt{-1}$. η_0 is the impedance of free space. The term $\exp\left(-k_0^2/\sigma^2\right)$ corresponds to a Gaussian pulse used to limit the bandwidth of incident wave. ξ^{-1} represents the inverse Fourier transform. If k_x, k_y are constant numbers, that means k_l is constant, so we can conclude that in the CTW wave different frequencies correspond different incident angles.

The x- and y- field components of the CTW wave can be calculated as,

$$\begin{aligned} E_x^{CTW} &= -\frac{k_y}{k_l}E_t^{CTW}, \quad E_y^{CTW} = \frac{k_x}{k_l}E_t^{CTW} \\ H_x^{CTW} &= \frac{k_x}{k_l}H_l^{CTW}, \quad H_y^{CTW} = \frac{k_y}{k_l}H_l^{CTW} \end{aligned}. \tag{2}$$

They can be added to the computational domain by using total-field/scattered-field method [1].

B. Formulations of the NWCS-SFDTD method

In the NWCS-SFDTD method, the field updating for one time step is performed using two

procedures. The relations between the field components of the novel weakly conditionally stable SFDTD scheme can be represented as,

$$([I]+[A])U^{n+\frac{1}{2}}=([I]+[B])U^{n} \tag{3}$$

$$([I]+[C])U^{n+1}=([I]+[D])U^{n+\frac{1}{2}}, \tag{4}$$

where $U^n=[E_x^n\ E_y^n\ E_z^n\ H_x^n\ H_y^n\ H_z^n]$ and $[I]$ denotes the unit matrix,

$$[A]=\begin{bmatrix}0 & \Delta t/2\varepsilon\square D_1\\ \Delta t/2\mu\square D_2^T & 0\end{bmatrix},[B]=\begin{bmatrix}0 & -\Delta t/2\varepsilon\square D_2\\ -\Delta t/2\mu\square D_1^T & 0\end{bmatrix} \tag{5}$$

$$[C]=\begin{bmatrix}0 & -\Delta t/2\varepsilon\square D_1^T\\ -\Delta t/2\mu\square D_2 & 0\end{bmatrix},[D]=\begin{bmatrix}0 & \Delta t/2\varepsilon\square D_2^T\\ \Delta t/2\mu\square D_1 & 0\end{bmatrix}, \tag{6}$$

$$[D_1]=\begin{bmatrix}0 & 0 & 0\\ 0 & 0 & D_x\\ 0 & D_y & 0\end{bmatrix},[D_2]=\begin{bmatrix}0 & 0 & 0\\ -2D_z & 0 & D_x\\ D_y & 0 & 0\end{bmatrix}, \tag{7}$$

where ε,μ represent the permittivity and permeability, Δt is the time step size. D_1^T, D_2^T represent the transpose of D_1, D_2, respectively. D_x, D_y, D_z are the first-order central difference operators along the x-, y- and z- axes.

Incorporating the optimization parameters α, β and γ [16, 17], and by inserting equations (5)-(7) into equations (3) and (4), we have,

$$E_x^{n+1/2}=E_x^n \tag{8a}$$

$$E_y^{n+1/2}=E_y^n+\frac{\gamma\Delta t}{\varepsilon\partial z}\partial H_x^n-\frac{\alpha\Delta t}{2\varepsilon\partial x}\partial\left(H_z^{n+1/2}+H_z^n\right), \tag{8b}$$

$$E_z^{n+1/2}=E_z^n-\frac{\beta\Delta t}{2\varepsilon\partial y}\partial\left(H_x^{n+1/2}+H_x^n\right), \tag{8c}$$

$$H_x^{n+1/2}=H_x^n+\frac{\gamma\Delta t}{\mu\partial z}\partial E_y^{n+1/2}-\frac{\beta\Delta t}{2\mu\partial y}\partial\left(E_z^{n+1/2}+E_z^n\right), \tag{8d}$$

$$H_y^{n+1/2}=H_y^n, \tag{8e}$$

$$H_z^{n+1/2}=H_z^n-\frac{\alpha\Delta t}{2\mu\partial x}\partial\left(E_y^{n+1/2}+E_y^n\right), \tag{8f}$$

for the first-half time-step. And

$$E_x^{n+1}=E_x^{n+1/2}-\frac{\gamma\Delta t}{\varepsilon\partial z}\partial H_y^{n+1/2}+\frac{\beta\Delta t}{2\varepsilon\partial y}\partial\left(H_z^{n+1}+H_z^{n+1/2}\right) \tag{9a}$$

$$E_y^{n+1}=E_y^{n+1/2}, \tag{9b}$$

$$E_z^{n+1}=E_z^{n+1/2}+\frac{\alpha\Delta t}{2\varepsilon\partial x}\partial\left(H_y^{n+1}+H_y^{n+1/2}\right), \tag{9c}$$

$$H_x^{n+1}=H_x^{n+1/2}, \tag{9d}$$

$$H_y^{n+1}=H_y^{n+1/2}-\frac{\gamma\Delta t}{\mu\partial z}\partial E_x^{n+1}+\frac{\alpha\Delta t}{2\mu\partial x}\partial\left(E_z^{n+1}+E_z^{n+1/2}\right), \tag{9e}$$

$$H_z^{n+1}=H_z^{n+1/2}+\frac{\beta\Delta t}{2\mu\partial y}\partial\left(E_x^{n+1}+E_x^{n+1/2}\right), \tag{9f}$$

for the second-half time-step. The control parameters α, β, and γ used in the above formulations contribute to a reduction of the numerical dispersion error.

It can be seen from these equations that only equations (8b)-(8d), (8f), (9a), (9c), (9e), and (9f) need to be solved. However, none of them can be updated directly, because they all include the unknown components on both sides of the equations. In the first-half time-step, updating of $E_y^{n+1/2}$ component needs the unknown $H_z^{n+1/2}$ components at the same time, so the $E_y^{n+1/2}$ component has to be updated implicitly. Substituting equation (8f) into equation (8b) and by appropriate rearrangement we can obtain the equation for $E_y^{n+1/2}$,

$$\begin{aligned}&E_y^{n+1/2}\big|_{i,j+1/2,k}-\frac{\alpha^2\Delta t^2}{4\varepsilon\mu\Delta x^2}\left(\begin{matrix}E_y^{n+1/2}\big|_{i+1,j+1/2,k}-\\ 2E_y^{n+1/2}\big|_{i,j+1/2,k}+E_y^{n+1/2}\big|_{i-1,j+1/2,k}\end{matrix}\right)\\ &=E_y^n\big|_{i,j+1/2,k}+\frac{\gamma\Delta t}{\varepsilon\Delta z}\left(H_x^n\big|_{i,j+1/2,k+1/2}-H_x^n\big|_{i,j+1/2,k-1/2}\right)\\ &-\frac{\alpha\Delta t}{\varepsilon\Delta x}\left(H_z^n\big|_{i+1/2,j+1/2,k}-H_z^n\big|_{i-1/2,j+1/2,k}\right)\\ &+\frac{\alpha^2\Delta t^2}{4\varepsilon\mu\Delta x^2}\left(E_y^n\big|_{i+1,j+1/2,k}-2E_y^n\big|_{i,j+1/2,k}+E_y^n\big|_{i-1,j+1/2,k}\right).\end{aligned} \tag{10}$$

Similarly, in the first-half time-step, updating of the $E_z^{n+1/2}$ component in equation (8c) needs the $H_x^{n+1/2}$ components at the same time. Substituting equation (8d) into equation (8c) we can obtain the equation for $E_z^{n+1/2}$,

$$\begin{aligned}&E_z^{n+1/2}\big|_{i,j,k+1/2}-\frac{\beta^2\Delta t^2}{4\varepsilon\mu\Delta y^2}\left(\begin{matrix}E_z^{n+1/2}\big|_{i,j+1,k+1/2}-\\ 2E_z^{n+1/2}\big|_{i,j,k+1/2}+E_z^{n+1/2}\big|_{i,j-1,k+1/2}\end{matrix}\right)\\ &=E_z^n\big|_{i,j,k+1/2}-\frac{\beta\Delta t}{\varepsilon\Delta y}\left(H_x^n\big|_{i,j+1/2,k+1/2}-H_x^n\big|_{i,j-1/2,k+1/2}\right)\\ &-\frac{\beta\gamma\Delta t^2}{2\varepsilon\mu\Delta y\Delta z}\left(\begin{matrix}E_y^{n+1/2}\big|_{i,j+1/2,k+1}-E_y^{n+1/2}\big|_{i,j+1/2,k}\\ -E_y^{n+1/2}\big|_{i,j-1/2,k+1}+E_y^{n+1/2}\big|_{i,j-1/2,k}\end{matrix}\right)\\ &+\frac{\beta^2\Delta t^2}{4\varepsilon\mu\Delta y^2}\left(E_z^n\big|_{i,j+1,k+1/2}-2E_z^n\big|_{i,j,k+1/2}+E_z^n\big|_{i,j-1,k+1/2}\right).\end{aligned} \tag{11}$$

After $E_y^{n+1/2}$ and $E_z^{n+1/2}$ are obtained, $H_x^{n+1/2}$ and $H_z^{n+1/2}$ can be explicitly updated by using

equations (8f) and (8d). The components $E_x^{n+1/2}$ and $H_y^{n+1/2}$ in the first-half time-step need not be solved. In the second-half time-step, updating of the E_x^{n+1} component needs the unknown H_z^{n+1} components at the same time. Substituting equation (9f) into equation (9a) we can obtain the equation for E_x^{n+1},

$$E_x^{n+1}\Big|_{i+1/2,j,k} - \frac{\beta^2\Delta t^2}{4\varepsilon\mu\Delta y^2}\left(\begin{array}{l} E_x^{n+1}\big|_{i+1/2,j+1,k} - \\ 2E_x^{n+1}\big|_{i+1/2,j,k} + E_x^{n+1}\big|_{i+1/2,j-1,k}\end{array}\right)$$
$$= E_x^{n+1/2}\Big|_{i+1/2,j,k} - \frac{\gamma\Delta t}{\varepsilon\Delta z}\left(H_y^{n+1/2}\Big|_{i+1/2,j,k+1/2} - H_y^{n+1/2}\Big|_{i+1/2,j,k-1/2}\right)$$
$$+\frac{\beta\Delta t}{\varepsilon\Delta y}\left(H_z^{n+1/2}\Big|_{i+1/2,j+1/2,k} - H_z^{n+1/2}\Big|_{i+1/2,j-1/2,k}\right)$$
$$+\frac{\beta^2\Delta t^2}{4\varepsilon\mu\Delta y^2}\left(\begin{array}{l} E_x^{n+1/2}\big|_{i+1/2,j+1,k} - \\ 2E_x^{n+1/2}\big|_{i+1/2,j,k} + E_x^{n+1/2}\big|_{i+1/2,j-1,k}\end{array}\right) . \quad (12)$$

In the same way by substituting equation (9e) into equation (9c) we can obtain the equation for E_z^{n+1},

$$E_z^{n+1}\Big|_{i,j,k+1/2} - \frac{\alpha^2\Delta t^2}{4\varepsilon\mu\Delta x^2}\left(\begin{array}{l} E_z^{n+1}\big|_{i+1,j,k+1/2} \\ -2E_z^{n+1}\big|_{i,j,k+1/2} + E_z^{n+1}\big|_{i-1,j,k+1/2}\end{array}\right)$$
$$= E_z^{n+1/2}\Big|_{i,j,k+1/2} + \frac{\alpha\Delta t}{\varepsilon\Delta x}\left(H_y^{n+1/2}\Big|_{i+1/2,j,k+1/2} - H_y^{n+1/2}\Big|_{i-1/2,j,k+1/2}\right)$$
$$-\frac{\alpha\gamma\Delta t^2}{2\varepsilon\mu\Delta x\Delta z}\left(\begin{array}{l} E_x^{n+1}\big|_{i+1/2,j,k+1} - E_x^{n+1}\big|_{i+1/2,j,k} \\ -E_x^{n+1}\big|_{i-1/2,j,k+1} + E_x^{n+1}\big|_{i-1/2,j,k}\end{array}\right)$$
$$+\frac{\alpha^2\Delta t^2}{4\varepsilon\mu\Delta x^2}\left(\begin{array}{l} E_z^{n+1/2}\big|_{i+1,j,k+1/2} \\ -2E_z^{n+1/2}\big|_{i,j,k+1/2} + E_z^{n+1/2}\big|_{i-1,j,k+1/2}\end{array}\right) . \quad (13)$$

After E_x^{n+1} and E_z^{n+1} are obtained, the components H_y^{n+1} and H_z^{n+1} can be updated straightforwardly by using equations (9e) and (9f). In the second-half time-step the components E_y^{n+1} and H_x^{n+1} need not be solved.

To solve equation (10), the periodic boundary condition needs to be combined. Because k_x, k_y are independent of frequency, there are no time delay in the $x-y$ plane, so in the first-half time-step the PBC for the CTW wave can be implemented in the same way as the PBC for normal incidence [1],

$$E_y^{n+1/2}\left(N_{x4}, j+\frac{1}{2}, k\right) = E_y^{n+1/2}\left(N_{x1}, j+\frac{1}{2}, k\right)e^{\tilde{j}k_xP_x} \quad (14)$$

$$E_z^{n+1/2}\left(i, N_{y4}, k+\frac{1}{2}\right) = E_z^{n+1/2}\left(i, N_{y1}, k+\frac{1}{2}\right)e^{\tilde{j}k_yP_y} , \quad (15)$$

$$E_z^{n+1/2}\left(N_{x4}, j, k+\frac{1}{2}\right) = E_z^{n+1/2}\left(N_{x1}, j, k+\frac{1}{2}\right)e^{\tilde{j}k_xP_x} , \quad (16)$$

$$H_x^{n+1/2}\left(i, N_{y1}-1, k+\frac{1}{2}\right) = H_x^{n+1/2}\left(i, N_{y4}-1, k+\frac{1}{2}\right)e^{-\tilde{j}k_yP_y} \quad (17)$$

$$H_z^{n+1/2}\left(N_{x1}-1, j, k+\frac{1}{2}\right) = H_z^{n+1/2}\left(N_{x4}-1, j, k+\frac{1}{2}\right)e^{-\tilde{j}k_xP_x} \quad (18)$$

$$H_z^{n+1/2}\left(i, N_{y1}-1, k+\frac{1}{2}\right) = H_z^{n+1/2}\left(i, N_{y4}-1, k+\frac{1}{2}\right)e^{-\tilde{j}k_yP_y} \quad (19)$$

where, N_{x1}, N_{x4}, N_{y1}, N_{y4} represent the nodes of electric fields on the unit cell boundary. $P_x = N_{x4}\Delta x$, $P_y = N_{y4}\Delta y$ are the dimensions of the unit cell in the x- and y- direction, respectively. In the second-half time-step the PBC for the CTW wave can be implemented similarly.

By substituting equations (14)-(19) into equation (10) we can get,

$$[\mathrm{M}]\,\vec{E}_y = \vec{d} \quad (20)$$

where $\vec{d}$ represents the right-hand vector of equation (10) and $\vec{E}_y$ is unknown in general. [M] is obtained from equation (10) for each column of E_y, so equation (10) can be written as,

$$\begin{bmatrix} n & m & & & \rho \\ m & n & m & & \\ & \cdots & \cdots & \cdots & \\ & & m & n & m \\ \tau & & & m & n \end{bmatrix}\begin{bmatrix} E_y^{n+1/2}\big|_{N_{x1},j+1/2,k} \\ E_y^{n+1/2}\big|_{N_{x1}+1,j+1/2,k} \\ \vdots \\ E_y^{n+1/2}\big|_{N_{x4}-1,j+1/2,k} \end{bmatrix} = \begin{bmatrix} d(N_{x1}) \\ d(N_{x1}+1) \\ \\ \vdots \\ d(N_{x4}-1) \end{bmatrix} \quad (21)$$

$$m = -\frac{\Delta t^2\alpha^2}{4\varepsilon\mu\Delta x^2}, n = 1+\frac{\Delta t^2\alpha^2}{2\varepsilon\mu\Delta x^2} , \quad (22)$$

where $\rho = m\cdot e^{-\tilde{j}k_xP_x}$, $\tau = m\cdot e^{\tilde{j}k_xP_x}$.

The coefficient matrix [M] is not a tridiagonal matrix, so it can't be solved with the efficient forward-elimination and backward-substitution method directly. By using the Sherman Morrison formula, two auxiliary linear problems are defined [18],

$$[N]\,\vec{E}_{y1} = \vec{d} \quad (23)$$

$$[N]\,\vec{E}_{y2} = \vec{v}_1 , \quad (24)$$

$$[N] = [M] - \vec{v}_1\vec{v}_2{}^T , \quad (25)$$

$$\vec{v}_1 = \begin{bmatrix} \rho^{1/2} & 0 & \cdots & 0 & \tau^{1/2} \end{bmatrix}^T , \quad (26)$$

$$\vec{v}_2 = \begin{bmatrix} \tau^{1/2} & 0 & \cdots & 0 & \rho^{1/2} \end{bmatrix} . \quad (27)$$

So the solution of equation (21) is obtained via,

$$\vec{E}_y = \vec{E}_{y1} + \varsigma \vec{E}_{y2} \quad (28)$$

$$\varsigma = -\frac{\vec{v}_2^{\,T} \vec{E}_{y1}}{1 + \vec{v}_2^{\,T} \vec{E}_{y2}} . \quad (29)$$

By observation, one can find that matrix [M] in equation (20) is related to matrix [N]. Because [N] is a tridiagonal matrix, the auxiliary linear problems can be solved efficiently by using forward-elimination and backward-substitution method. Equations (11), (12), and (13) can be solved in the same way.

From the equations derived above, it can be seen that at each time step, the proposed method requires solution of four implicit updates and four explicit updates, while it needs to solve six implicit updates and six explicit updates in the ADI-SFDTD scheme. So we can find, the implementation of the NWCS-SFDTD method is simpler than the ADI-SFDTD method.

In the NWCS-SFDTD method the maximum time-step size is only determined by one spatial increment as it is in [14]. This is especially useful when the simulated structure has a fine-scale dimension in one or two directions. A small spatial increment can be used in the direction with fine scale and a larger spatial increment can be used in the direction with coarse scale. If we perform the implicit-difference scheme in the direction with a larger spatial increment, the time-step size is thus determined by the larger spatial increments. For example, the size of the structure in the z-direction is larger than those in the x- and y-directions. By setting $\Delta z = 10\Delta y = 10\Delta x$, the maximum time-step size meeting the stability condition of the NWCS-SFDTD algorithm can be determined as $\Delta t = \Delta z / c$, while the maximum time-step size for the conventional SFDTD method is $\Delta t = \dfrac{1}{c\sqrt{\Delta x^{-2} + \Delta y^{-2} + \Delta z^{-2}}} = \dfrac{\Delta z}{c\sqrt{201}}$. As a result, computational resources can be saved considerably.

III. NUMERICAL RESULTS

In this section a numerical example is presented to demonstrate the proposed NWCS-SFDTD method. Simulation results are carried out using the NWCS-SFDTD method, the conventional SFDTD method and the ADI-SFDTD method for comparison.

In the example, it is applied to calculate the reflection coefficient of EBG structure, the analyzed model is shown in Fig. 1. The structure is a periodic array of metallic squares with thin slots embedded in a dielectric slab. The dielectric slab has relative permittivity $\varepsilon_r = 4.0$. The physical dimensions of the geometry are $w = 5\text{mm}$, $d = 2.5\text{mm}$, $h = 25\text{mm}$. The sizes of the thin slots are 0.5mm. The space increments are $\Delta x = \Delta y = \Delta z/5 = 0.5$ mm. The computational domain is truncated by 16-layer PML in the z direction. So it contains 20×20×102 cells. The CTW wave is introduced into the computational domain, with the transverse wave-number k_x ranges from 0 m^{-1} to 200 m^{-1}. To satisfy the stability condition of the FDTD algorithm, the time-step size for the conventional SFDTD is $\Delta t \le 1.16$ ps, and the time-step size for the NWCS-SFDTD algorithm is only determined by increment Δz, that is $\Delta t \le 8.33$ ps. So in the simulation, the time-step size for the SFDTD method is kept constant $\Delta t = 1.16$ ps, while in the ADI-SFDTD and the NWCS-SFDTD method two time-step sizes are chosen, namely, 1.16 ps and 8.33 ps.

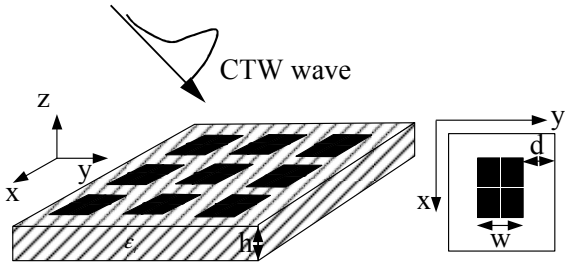

Fig. 1. The geometry of the numerical example.

Figure 2 shows the reflection coefficient of the EBG structure with the time-step size 1.16 ps for the conventional SFDTD, the NWCS-SFDTD, and the ADI-SFDTD method, respectively. It can be seen from these figures that both the proposed NWCS-SFDTD method and the ADI-SFDTD method agree well with the conventional SFDTD method, which means when the time-step size is small both the NWCS-SFDTD method and the ADI-SFDTD method have high accuracy.

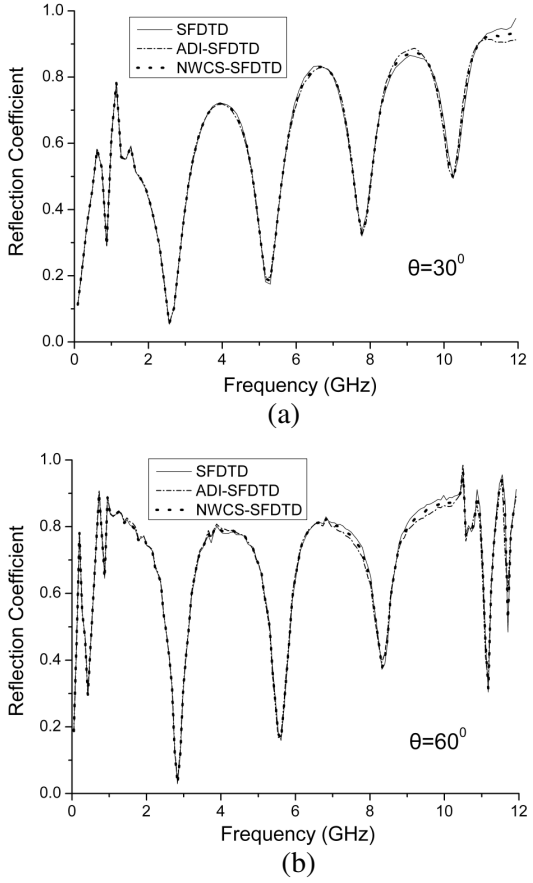

Fig. 2. Reflection coefficients for the conventional SFDTD (Δt = 1.16 ps), the NWCS-SFDTD (Δt = 1.16 ps), and the ADI-SFDTD (Δt = 1.16 ps) method for $\theta = 30^{o}$ and $\theta = 60^{o}$.

When the time-step size increases to 8.33 ps, the results are shown in Fig. 3. From Fig. 3 we can see when the time-step size increases both the ADI-SFDTD method and the proposed method have a deviation from the conventional SFDTD method. It is also shown that the discrepancy is larger at high frequencies than low frequencies. However, the deviation of the NWCS-SFDTD method is smaller than the ADI-SFDTD method. It is apparent that the proposed method has higher accuracy than the ADI-SFDTD method.

To reduce the numerical dispersion error, we employ the improved NWCS-SFDTD method with dispersion control parameters [19],

$$\alpha = \frac{\Delta x \tan\left(\frac{1}{2}ck\Delta t\right)}{c\Delta t \sin\left(\frac{1}{2}k\Delta x\right)},\quad \gamma = \frac{\Delta z \tan\left(\frac{1}{2}ck\Delta t\right)}{c\Delta t \sin\left(\frac{1}{2}k\Delta z\right)},\quad \beta = 1. \quad (30)$$

So when the time-step size is 8.33 ps, $\alpha = \gamma = 1.0246, \beta = 1$ are obtained. It can be seen from Fig. 4 that the results with dispersion control parameters reach a good agreement with the conventional SFDTD method.

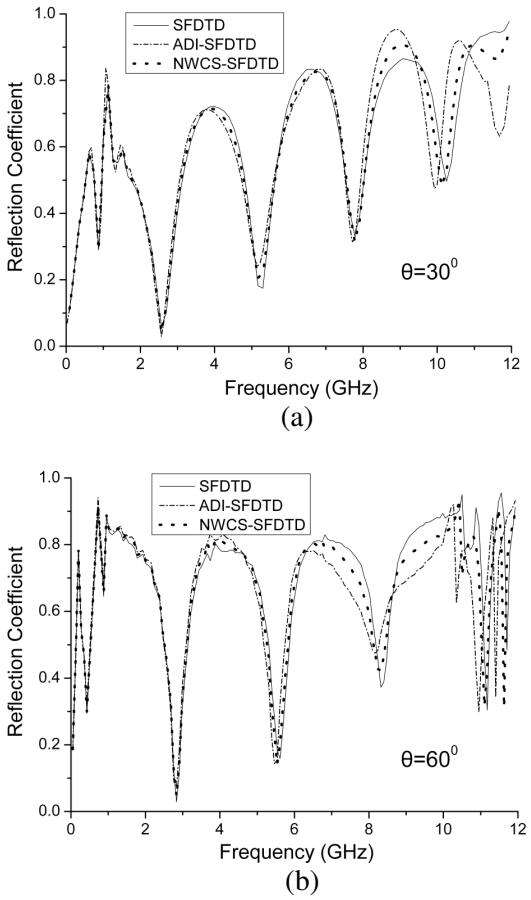

Fig. 3. Reflection coefficients for the conventional SFDTD (Δt = 1.16 ps), the NWCS-SFDTD (Δt = 8.33 ps) and the ADI-SFDTD (Δt = 8.33 ps) method for $\theta = 30^{o}$ and $\theta = 60^{o}$.

Finally, we mention the computational efficiency of the proposed NWCS-SFDTD method. On a Core2 2.4-GHz machine, it took the conventional SFDTD method 67446.6 seconds and the NWCS-SFDTD method (with the time-step size 8.33 ps) 17207.4 seconds to run the same simulation, which is 25737.3 seconds in the ADI-SFDTD method. So compared with the ADI-SFDTD method, the proposed method has higher efficiency. The CPU running time for this method is about 2/3 of the ADI-SFDTD method.

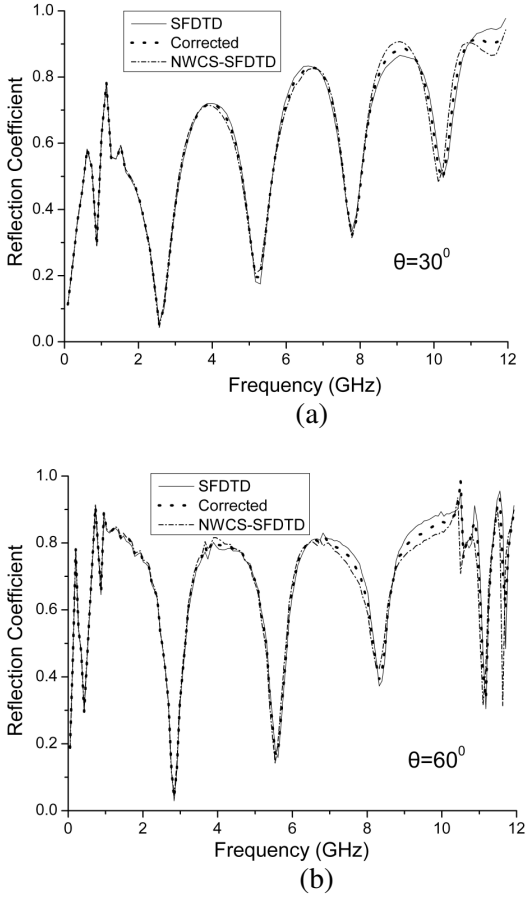

Fig. 4. Reflection coefficients calculated by the NWCS-SFDTD method (Δt = 8.33 ps) and the improved method with dispersion control parameters for $\theta = 30^{o}$ and $\theta = 60^{o}$.

IV. CONCLUSION

In this paper, we present a novel weakly conditionally stable SFDTD method to solve periodic structures at oblique incidence. Numerical results indicate that the proposed method is accurate and efficient. The CPU time for the proposed method can be reduced to about 2/3 of the ADI-SFDTD method. For the same time-step size, the proposed method not only has higher efficiency than the ADI-SFDTD method, but also higher accuracy.

ACKNOWLEDGMENT

This work was supported by Chinese National Science Foundation under Grant No. 60971063.

REFERENCES

[1] A. Taflove and S. Hagness, *Computational Electrodynamics: The Finite-Difference Time-Domain Method*, 2nd ed. Boston, MA: Artech House, 2000.

[2] B. Henin, A. Elsherbeni, F. Yang, and V. Demir, "FDTD formulation for the scattering from metamaterial under obliquely incident plane," *26th Annual Review of Progress in Applied Computational Electromagnetics (ACES)*, pp. 474-478, 2010.

[3] J. Wang, T. Zhao, J. Song, and T. Kamgaing, "Modeling of multilayered media for oblique incidence using effective medium theory," *28th Annual Review of Progress in Applied Computational Electromagnetics (ACES)*, pp. 812-817, 2012.

[4] T. Maruyama, Y. Oda, J. Shen, N. Tran, and H. Kayama, "The design of reflectarray using dual resonant characteristics of mushroom like structure," *28th Annual Review of Progress in Applied Computational Electromagnetics (ACES)*, pp. 780-785, 2012.

[5] T. Ikiz and M. K. Zateroglu, "Diffraction of obliquely incident plane waves by an impedance wedge with surface impedcances being equal to the intrinsic impedance of the medium," *Applied Computational Electromagnetics Society (ACES) Journal*, vol. 26, no. 3, pp. 199-205, 2011.

[6] P. Harms, R. Mittra, and K. Wai, "Implementation of the periodic boundary condition in the finite-difference time-domain algorithm for FSS structures," *IEEE Trans. Antennas Propagat.*, vol. 42, pp. 1317-1324, 1994.

[7] Y. Mao and B. Chen, "Parallel implementation of the split-field FDTD method for the analysis of periodic structure," *IEEE the 8th International Symposium on Antennas Propagation and EM Theory Proceeding*.

[8] A. Aminian and R.-S. Yahya, "Spectral FDTD: a novel technique for the analysis of oblique incident plane wave on periodic structures," *IEEE Trans. Antennas Propagat.*, vol. 54, pp. 1818-1825, 2006.

[9] Y.-F. Mao, B. Chen, H.-L. Chen, and Q. Wu, "Unconditionally stable SFDTD algorithm for solving oblique incident wave on periodic structures," *IEEE Microw. Wireless Compon. Lett.*, vol. 19, pp. 257-259, 2009.

[10] Y. Wakabayashi, J. Shibayama, J. Yamauchi, and H. Nakano, "A locally one-dimensional finite difference time domain method for the analysis of a periodic structure at oblique incidence," *Radio Science*, vol. 46, pp. 1-9, 2011.

[11] I. Ahmed and Z. Chen, "Error reduced ADI-FDTD methods," *IEEE Antennas and Wireless Propagat. Lett.*, vol. 4, pp. 323-325, 2005.

[12] J. Chen and A. Zhang, "A subgridding scheme based on the FDTD method and HIE-FDTD method," *The Applied Computational Electromagnetic Society (ACES) Journal*, vol. 26, no. 1, Jan. 2011.
[13] Y. Mao, B. Chen, et al., "WCS-FDTD algorithm for periodic structures," *IEEE Antennas and Wireless Propagat. Lett*., vol. 10, pp. 1236-1238, 2011.
[14] J. Chen and J. Wang, "A novel WCS-FDTD method with weakly conditional stability," *IEEE Trans. Electromagn. Compat.*, vol. 49, no. 2, pp. 419-426, May 2007.
[15] J. Chen and J. Wang, "A novel body-of –revolution finite-difference time-domain method with weakly conditional stability," *IEEE Microw. Wireless Compon. Lett.*, vol. 18, no. 6, pp. 377-379, June 2008.
[16] A.-P. Zhao, "Two special notes on the implementation of the unconditionally stable ADI-FDTD method," *Microwave and Optical Tech. Lett.*, vol. 33, no. 4, pp. 273-277, 2002.
[17] H. Zheng and K. Leung, "An efficient method to reduce the numerical dispersion in the ADI-FDTD," *IEEE Trans. Microw. Theory Tech.*, vol. 53, no. 7, pp. 2295-2301, July 2005.
[18] J.-W. Thomas, *Numerical Partial Differential Equations: Finite Difference Methods*, Berlin, Germany: Springer Verlag, 1995.
[19] M. Wang, Z. Wang, and J. Chen, "A parameter optimized ADI-FDTD method," *IEEE Antennas Wireless Propag. Lett.*, vol. 2, pp. 118-121, May 2003.

Yun-Fei Mao was born in Zhejiang province, China, in 1984. He received the B. S. degrees, the M.S. degree and the Ph.D. degree in Electric Systems from Nanjing Engineering Institute, Nanjing, China, in 2006, 2009, and 2013 respectively. He is currently working in China Satellite Maritime Tracking and Control Department, Yuan Wang, Jiangyin 214400, China. His research interests include computational electromagnetic and electro-magnetic tracking.

Bin Chen was born in Jiangsu, China, in 1957. He received the B.S. and M.S. degrees in Electrical Engineering from Beijing Institute of Technology, Beijing, China, in 1982 and 1987, respectively, and the Ph.D. degree in Electrical Engineering from Nanjing University of Science and Technology, Nanjing, China, in 1997. Currently, he is a Professor at National Key laboratory on Electromagnetic Environment and electro-optical Engineering, PLA University of Science and Technology. His research includes computational electromagnetics, EMC and EMP.

Xiao-Xu Yin was born in Hubei province, China, in 1978. He received the B.S. degrees in Wuhan university, Wuhan, China, in 1999. He is currently working in China Satellite Maritime Tracking and Control Department, Yuan Wang, Jiangyin 214400, China. His research interests include electromagnetics and electromagnetic tracking.

Jian Chen was born in Jiangsu province, China, in 1976. He received He received the B.S. North Western Industry University, Xi'an, China, in 1999. He is currently working in China Satellite Maritime Tracking.